

1  
2  
3  
4  
5  
6  
7  
8  
9  
10  
11  
12  
13  
14  
15  
16  
17  
18  
19  
20

Received Date : 28-Mar-2016

Revised Date : 10-Jun-2016

Accepted Date : 01-Jul-2016

Article type : Original Article

**High Throughput Quantitative Method for Assessing Coaggregation among Oral Bacterial Species**

Elizabeth Levin-Sparenberg<sup>1</sup>, Jae Min Shin<sup>2</sup>, Erica Hastings<sup>3</sup>, Melissa Freeland<sup>1</sup>, Hannah Segaloff<sup>1</sup>,  
Alexander H. Rickard<sup>1</sup>, Betsy Foxman<sup>1</sup>

<sup>1</sup> Epidemiology Department, School of Public Health, University of Michigan, Ann Arbor, Michigan

<sup>2</sup> Department of Periodontics and Oral Medicine, University of Michigan School of Dentistry, Ann Arbor,  
Michigan

<sup>3</sup> Department of Chemical Engineering, University of Michigan, Ann Arbor, Michigan

**Corresponding author:**

Betsy Foxman, PhD

M5108 SPH II

This is the author manuscript accepted for publication and has undergone full peer review but has not been through the copyediting, typesetting, pagination and proofreading process, which may lead to differences between this version and the [Version of Record](#). Please cite this article as [doi: 10.1111/lam.12622](https://doi.org/10.1111/lam.12622)

21 1415 Washington Heights

22 Ann Arbor, Michigan 48109-2029

23 [bfoxman@umich.edu](mailto:bfoxman@umich.edu)

24

25

26

27

28

29 Abbreviated Title: Coaggregation: High-throughput Assessment Method

30 **Significance and Impact of the Study**

31 Coaggregation between bacterial species is integral to multi-species biofilm development.  
32 Difficulties in rapidly and reproducibly identifying and quantifying coaggregation have limited  
33 mechanistic studies. This paper demonstrates two complementary quantitative methods to screen for  
34 coaggregation. The first approach uses a microplate-based high-throughput approach and the other  
35 uses a FlowCam™ device. The microplate-based approach enables rapid detection of coaggregation  
36 between candidate coaggregating pairs of strains simultaneously while controlling for variation between  
37 replicates. The FlowCam™ approach allows for in-depth analysis of the rates of coaggregation and size of  
38 aggregates formed.

39

40

41

42

43

44

45

46

47 **Abstract**

48 This paper describes a high throughput method that relies upon a microplate reader to score  
49 coaggregation 60 minutes post mixing, and use of a high-speed real-time imaging technology to describe  
50 the rate of coaggregation over time. The results of visual, microplate, and FlowCam™ aggregation scores  
51 for oral bacteria *Streptococcus gordonii*, *Streptococcus oralis*, and *Actinomyces oris*, whose ability to  
52 coaggregate are well characterized, are compared. Following mixing of all possible pairs, the top fraction  
53 of the supernatant was added to a microplate to quantify cell-density. Pairs were also passed through a  
54 flow cell within a FlowCam™ to quantify the rate of coaggregation of each pair. Results from both the  
55 microplate and FlowCam™ approaches correlated with corresponding visual coaggregation scores and  
56 microscopic observations. The microplate-based assay enables high throughput screening, whereas the  
57 FlowCam™-based assay validates and quantifies the extent that autoaggregation and coaggregation  
58 occur. Together these assays open the door for future in-depth studies of autoaggregation and  
59 coaggregation among large panels of test strains.

60

61

62 Keywords: Coaggregation, *Actinomycetes*, Biofilms, Biotechnology, *Streptococci*

63

64

65

66 **Introduction**

This article is protected by copyright. All rights reserved

67 Coaggregation is defined as the highly specific recognition and adherence of different species of  
68 bacteria with each other (Kolenbrander 1988; Rickard et al. 2003). Coaggregation typically occurs as a  
69 consequence of the expression of protein adhesins on the cell-surface of one bacterial species, and  
70 complementary polysaccharide-containing receptors expressed on the surface of the other bacterial  
71 species (Kolenbrander 1988; Rickard et al. 2003).

72 Coaggregation interactions are important for the development of multi-species biofilms (e.g.  
73 dental plaque). It contributes to biofilm development via at least two mechanisms: i) free floating  
74 planktonic cells of one species specifically recognize cells of another species type and co-adhere to the  
75 developing biofilm, and/or ii) bacterial cells of a planktonic species recognize and coaggregate with cells  
76 of another species within an established biofilm community (Rickard et al. 2003; Kolenbrander et al.  
77 2010). It is likely that these interactions are important for adherence and colonization of bacteria to a  
78 variety of biotic and abiotic surfaces, and provide selective advantages against non-coaggregated  
79 bacterial species contained within a biofilm (Kolenbrander et al. 1990; Busscher and Van Der Mei 1995;  
80 Burmølle et al. 2006; Kolenbrander et al. 2010).

81 The oral microorganisms *Streptococcus oralis*, *Streptococcus gordonii* and *Actinomyces oris*  
82 strongly coaggregate and are considered early colonizers in the process of dental plaque formation.  
83 (Kolenbrander 2000). Early colonizers anchor the biofilm to the substratum surface and thereby  
84 contribute to recalcitrance of the biofilm to removal (Busscher and Van Der Mei 1995). For example, the  
85 presence of *A. oris* greatly reduces the ability of the *S. oralis* to be removed by shear force when  
86 compared with direct attachment of *S. oralis* to the pellicle (proteinaceous conditioning film formed on  
87 the tooth surface) (Busscher and Van Der Mei 1995). Furthermore, early colonizers provide a  
88 foundation for other species to adhere, forming a mature biofilm community (Busscher and Van Der Mei  
89 1995). Through autoaggregation (aggregation within a single species) or coaggregation, organisms can  
90 individually and collectively obtain increased resistance towards antimicrobials and shear forces,  
91 communicate via cell-cell signaling, and share nutrients (Kinder and Holt 1994; Watnick and Kolter 2000;  
92 Rickard et al. 2003). Research using model dental plaque systems has shown nutritionally mutualistic  
93 relationships occurring between coaggregating organisms (Bradshaw 1994; Palmer et al. 2001). For  
94 example, *A. oris* and *S. oralis* displayed limited to no growth when grown in monoculture with saliva as  
95 the nutrient source, but thrived when allowed to coaggregate (Palmer 2001).

96 Traditionally, coaggregation is assessed using a visual scoring system based on the size of the  
97 coaggregates and turbidity of the supernatant fluid (Cisar et al. 1979; Gilbert et al. 2002; Vornhagen et  
98 al. 2013). However, as visual scoring is only semi-quantitative, it is subject to inconsistency and bias in  
99 scoring (Busscher and Van Der Mei 1995). Another method, measuring the percent change in optical  
100 density, provides a quantitative assessment and greatly improves reliability and reproducibility.  
101 However, current methods are not amenable to screening of larger numbers of samples simultaneously  
102 (Ikegami et al. 2004; Ledder et al. 2008; Nagaoka et al. 2008; Arzmi et al. 2015) and these technological  
103 insufficiencies have limited the in depth study of coaggregation (Katharios-Lanwermeier et al. 2014).  
104 The ability to include multiple replicates in a single experiment is highly desirable, as there may be strain  
105 variations in coaggregation requiring multiple crosses to determine if the observed coaggregation occurs  
106 generally between two species. Furthermore, because bacterial coaggregation is sensitive to a variety of  
107 influences including presence of chelating agents (Taweechaisupapong and Doyle 2000), temperature  
108 (Postollec et al. 2005), growth media, and pH (Min et al. 2010), and growth phase of the batch culture  
109 cells (Rickard et al. 2000), high throughput methods would be highly desirable to improve reproducibility  
110 of results.

111 Cognizant of these issues, we developed a quantitative method for high throughput screening  
112 for coaggregation among bacterial species. Our high throughput method allows for simultaneous  
113 analysis of multiple replicates so that experimental variation is reduced and possible subjective bias is  
114 minimized. This method's accuracy as a preliminary screening tool was validated using confocal  
115 microscopy and a recently developed approach using FlowCam™ technology (Segaloff 2014). A  
116 FlowCam™ is a dynamic imaging particle analyzer that examines fluid through a microscope and  
117 captures images of the particles as they are pumped through a flow cell via a computer controlled  
118 syringe pump. Specifically, a FlowCam™ characterizes the particles using a variety of measurements  
119 such as area-based diameter. It has been used in a variety of different industries including aquatic  
120 research, algae technology, waste management, pharmaceutical, and oil and gases for purposes such as  
121 monitoring algae for biofuels, quantifying protein aggregates in pharmaceuticals, and analyzing drilling  
122 products (<http://www.fluidimaging.com/>). In practice, the high throughput method can be used to  
123 screen a large panel of test strains for potential coaggregation. Ideally, strains giving a positive result  
124 with the high throughput method would then be tested further using either confocal microscopy or  
125 FlowCam™.

126 Without a high throughput, quantitative method for assessing coaggregation, it is difficult to  
127 explore the importance of coaggregation for the development of biofilms. A better understanding of  
128 coaggregation can provide a deeper knowledge of how organisms interact and biofilms form. For  
129 example, the presence of biofilms can result in the corrosion of sewer pipes. An improved  
130 understanding of if and how organisms coaggregate in these biofilms could help in developing strategies  
131 to reduce the detrimental effects of species in biofilms on pipe surfaces (Jensen et al. 2016). A high  
132 throughput screening method would also be of interest to the dental research community as identifying  
133 coaggregation between oral bacterial species (beyond those already known) could be an important step  
134 in developing a fuller understanding of dental plaque development (Kolenbrander et al. 1990).  
135 Coaggregation may also be an important mechanism through which pathogens interact with the host  
136 microbiota. Younes et al. demonstrated a rapid anti-pathogen effect of probiotic lactobacilli with toxic  
137 shock syndrome toxin 1-producing *Staphylococcus aureus* strains as a result of coaggregation (Younes et  
138 al. 2012). High throughput studies of coaggregation between organisms could be useful in identifying  
139 probiotic species.

## 140 **Results and Discussion:**

### 141 **High throughput quantitative method increases validity and reliability of results**

142 Three strains of oral bacteria were used: *Streptococcus oralis* 34, *Streptococcus gordonii* DL1,  
143 and *Actinomyces oris* T14V. *S. gordonii* is a primary colonizer in dental plaques and was previously  
144 found to coaggregate with both *A. oris* T14V and *S. oralis* 34 (Cisar et al. 1979). All possible pairwise  
145 combinations of these three strains were tested, resulting in six potential coaggregative or  
146 autoaggregative pairings. Coaggregation was first assessed in a low throughput format and scored using  
147 the visual scoring system developed by Cisar and colleagues (Cisar et al. 1979). As shown in Figure 1A,  
148 the maximum visual coaggregation (score = 4) is easily distinguished from no coaggregation (score = 0),  
149 but visual intermediate scoring is more subjective and as a consequence is less reproducible.

150 Using the microplate-based approach with OD 620 nm, it was determined that *S. gordonii* DL1 +  
151 *A. oris* T14V, *S. oralis* 34 + *A. oris* T14V, and *S. oralis* 34 + *S. gordonii* DL1 all strongly coaggregated (Figure  
152 1B). No autoaggregation was detected for *S. oralis* 34 or *S. gordonii* DL1. Some autoaggregation was  
153 observed for *A. oris* T14V, although the OD did not differ significantly from that of non-autoaggregating  
154 strains.

155 Within each micro-plate run, pairs were assayed in triplicate. The average coefficient of  
156 variation (standard error / mean) for the triplicates was 14% with a median of 9%. The coefficient of  
157 variations differed by specific crosses with autoaggregation by *A. oris* being the most variable (ranging  
158 from 1-66%). An increase in the coefficient of variation for coaggregation was also observed when *A.*  
159 *oris* was a component of a coaggregating pair.

160 Many factors contribute to between run variations: bacteria are harvested from separately  
161 grown batch cultures, which may differ slightly in length of growth time, exact nutrient content and pH  
162 of media, pH of buffers used for washing and re-suspension, number of times strain has been passaged  
163 before current growth, and natural biological variation. To minimize these variations, bacteria of a given  
164 species were harvested from the same batch culture, although some variation might remain due to the  
165 slight variations in timing between admixture and measurement, and true biologic variation in the  
166 amount of autoaggregation occurring within each species of a given candidate coaggregative pairing.

167 Between run and within run variation highlight the need for multiple replicates of each  
168 candidate coaggregative pair in addition to replicates of each strain on its own (to assess  
169 autoaggregation) within a single run. This is easily possible using the high-throughput 96-well plate  
170 method. Quantitatively comparing coaggregative and autoaggregative behavior within a single run also  
171 enables more accurate assessments of coaggregation by controlling for any autoaggregation that may  
172 occur, and multiple replicates of all strains and strain pairs allow for construction of confidence intervals  
173 around the mean OD value for a given strain or strain pair.

#### 174 **FlowCam™ Technology can measure particle sizes and quantify rate of coaggregation**

175 FlowCam™ technology was used to validate the high-throughput 96-well plate system, providing  
176 an in-depth analysis of the rates of coaggregation, and visual and quantitative assessment of the size of  
177 aggregates formed (Segaloff et al. 2014). The average particle size per minute increased over time for  
178 all three coaggregative pairings (Figure 2). By minute three (two minutes post-mixing) all coaggregating  
179 strains experienced a statistically significant increase in average particle area per minute as calculated  
180 using area-based diameter. Strong coaggregation occurred when *S. gordonii* and *A. oris* were combined,  
181 with particles averaging 212  $\mu\text{m}^2$  per minute and reaching as large as 3,800  $\mu\text{m}^2$  in area. The  
182 coaggregation between *S. oralis* and *S. gordonii* was not as strong. Particle sizes averaged 122  $\mu\text{m}^2$  by  
183 the final minute of data collection and reached a maximum area of approximately 2,950  $\mu\text{m}^2$ , but many

184 cells did not coaggregate and remained in suspension. This variation in coaggregation between this pair  
185 resulted in large confidence intervals around each time point. *S. oralis* and *A. oris* coaggregated strongly  
186 with particle sizes averaging 215  $\mu\text{m}^2$  in area by minute two and reaching sizes as large as 3,180  $\mu\text{m}^2$ . In  
187 the autoaggregation assays, the average area of *A. oris* particles (83  $\mu\text{m}^2$ ) was significantly larger than  
188 those of *S. oralis* (35  $\mu\text{m}^2$ ) and *S. gordonii* (51  $\mu\text{m}^2$ ), indicating strong autoaggregation in this species.  
189 Here, the use of FlowCam™ allowed for quantification of rates of coaggregation and measurement of  
190 the particle size associated with coaggregation. Results from FlowCam™ correlated well with the results  
191 of the high throughput screen, with coaggregation indicated by increases in particle size over time  
192 following the addition of the second organism and autoaggregation indicated by larger particle sizes.  
193 FlowCam™ was more useful for detecting autoaggregation than the high throughput screening method  
194 on its own, which did not show a statistically significant difference between autoaggregating and non-  
195 autoaggregating strains. These results validate the use of the high throughput method as an initial  
196 screening step to be followed up with a more confirmatory assay such as FlowCam™ or confocal  
197 microscopy.

#### 198 **Confocal microscopy confirms presence of coaggregation**

199 As a further confirmation, the strains were stained using Syto-9 (green) or Syto-61 (red) nucleic  
200 acid stains before crossing them for coaggregation, and then visualized using a confocal microscope  
201 (Figure 3). Confocal microscopy images confirmed that *S. oralis* and *S. gordonii* do not autoaggregate  
202 (Figure 3, A and C). Visualization of *A. oris* alone confirmed strong autoaggregative behavior (Figure 3B).  
203 This was not immediately apparent from initial absorbance readings from the high throughput screening  
204 method because autoaggregation was not followed by immediate sedimentation (Figure 1B). This  
205 finding is consistent with previous reports. Koop and colleagues showed autoaggregation without  
206 associated sedimentation could be missed by spectrophotometry (Koop et al. 1989), highlighting the  
207 importance of using a combination of methods for detection. The high-throughput 96-well plate  
208 method is most appropriately applied as a screen for potentially coaggregating pairs from a large pool of  
209 candidates. Potentially coaggregating pairs should be further evaluated using FlowCam™ or confocal  
210 microscopy, ideally both. Moreover, if coaggregation is suspected, autoaggregation should be ruled out.

211 *S. oralis* + *S. gordonii* showed moderate coaggregation (Figure 3D) while *S. gordonii* + *A. oris*  
212 (Figure 3E) and *S. oralis* + *A. oris* (Figure 3F) showed strong coaggregation. *S. oralis* and *S. gordonii*  
213 appeared to coaggregate in a more even manner, suggesting absence of autoaggregation within the two



214 species (Figure 3D), while *S. oralis* + *A. oris* and *S. gordonii* + *A. oris* showed clumps of the same color  
215 (red or green) indicating strong autoaggregative behavior by *A. oris* (Figure 3, E and F).

## 216 **Summary**

217 Focusing on the interactions between three well-documented coaggregating strains of oral  
218 bacteria, we demonstrated that coaggregation can be quantified, and the kinetics of coaggregation and  
219 the size of coaggregates formed can be measured. The microplate-based assay enables high throughput  
220 screening to identify potentially coaggregating strains, whereas the FlowCam-based assay validates and  
221 quantifies the extent that aggregation and coaggregation occur. In the absence of FlowCam™, or in  
222 combination with its use, confocal microscopy is a useful tool for confirming the presence or absence of  
223 coaggregation following screening of a large panel of strains with the high throughput method.  
224 Together these assays open the door for in-depth studies of aggregation and coaggregation among large  
225 panels of test strains.

## 226 **Materials and Methods:**

### 227 **Growth Conditions**

228 *S. oralis* 34 and *S. gordonii* DL1 were incubated aerobically with CO<sub>2</sub> at 37°C in Schaedler's broth  
229 for 24 hours. *A. oris* T14V was incubated aerobically with CO<sub>2</sub> at 37°C in Brain Heart Infusion broth for  
230 48 hours. Cells were harvested from batch culture through centrifugation for 12.5 minutes at 3,000 X g  
231 and then washed 3 times in coaggregation buffer (Cisar et al. 1979; Rickard et al. 2000). After each  
232 centrifugation step, the supernatant was discarded and the pellet was re-suspended in coaggregation  
233 buffer. The washed pellets were then suspended in coaggregation buffer to achieve an optical density  
234 at 600 nm of 1.5 (±0.1).

### 235 **Coaggregation and Autoaggregation assays**

236 Coaggregation and autoaggregation were first assessed using a visual coaggregation assay  
237 developed by Cisar et al. where visual scores ranged from 0 (no visible aggregates in the suspension) to  
238 4 (large aggregates form and settle leaving a clear supernatant) (Cisar et al. 1979). To assess  
239 coaggregation between two strains, 200 µl of each bacterial suspension were combined in a glass  
240 culture tube. To assess autoaggregation 400 µl of the single bacterial suspension as placed in a glass

241 culture tube. The culture tubes were then vortexed for ten seconds and rolled gently for an additional  
242 30 seconds (Rickard et al. 2000). Each pair was assayed in triplicate.

243 Samples were allowed to sit 60 minutes to let coaggregates settle to the bottom of the tube.  
244 Any changes in visual coaggregation score following the 60-minute time period were documented. This  
245 endpoint was selected after initial testing of the supernatant at 30 minute time intervals over 3 hours;  
246 60 minutes was ideal for good separation between coaggregating and non-coaggregating strains. One  
247 hundred microliters of supernatant were removed from each sample and placed in a 96 well flat-bottom  
248 plate. Absorbance of the supernatant was measured at 620 (A) using a PerkinElmer 2030 workstation  
249 (PerkinElmer Life and Analytical Sciences, Turku, Finland). Mean OD and associated 95% confidence  
250 intervals were calculated over all trials for each of the strain pairs and for each strain alone. Because  
251 strains were set to the same optical density (1.5) before they were combined, an expected value for the  
252 combined pair was calculated based on the average experimental OD of the two components. The  
253 mean OD, 95% confidence interval, minimum and maximum for each pair was then compared with the  
254 calculated expected value for the pair. Coaggregation was suspected when the expected value was  
255 above the upper limit for the 95% confidence interval and was considered when the mean OD was  
256 below the expected value. In all cases meeting these criteria, further screening was conducted using  
257 FlowCam™ and confocal microscopy.

258 As an additional visual test of autoaggregation and coaggregation between strains, 300 µl of  
259 each bacterial suspension in coaggregation buffer were stained with either Syto-9 (green: Excitation:  
260 488, Emission: 503) or Syto-61 (red: Excitation: 561, Emission: 645) nucleic acid stains (Invitrogen,  
261 Carlsbad, CA, USA). Each bacterial suspension was incubated for 30 minutes at room temperature to  
262 allow staining of the cells. Cells were washed three times with coaggregation buffer and collected by  
263 centrifugation, as mentioned above. Each bacterial strain was re-suspended in coaggregation buffer and  
264 combined for coaggregation. For autoaggregation studies, Syto-9 and Syto-61 stained cells of that  
265 species were mixed together. Twenty microliters of each sample were added to the slide and viewed  
266 under the microscope. The entire droplet was scanned and a minimum of three representative fields of  
267 view were captured for each pair and for each strain alone using Leica confocal laser scanning  
268 microscopy (CLSM, SPE, Leica, IL, USA) with a HCX PL APO 40X/0.85 CORR CS objective. Staining and  
269 microscopy were repeated twice to ensure consistency of results.” Once the microscopy images were

270 taken, the image files were rendered using Imaris (Bitplane, Zurich, Switzerland) computer imaging  
271 software.

## 272 **FlowCam™ Imaging and Quantification of Coaggregation**

273 To confirm the results of our findings, coaggregation was quantified using FlowCam™  
274 technology (Fluid Imaging Technologies, ME, USA). *S. oralis* 34, *S. gordonii* DL1 and *A. oris* T14V were  
275 harvested from batch cultures and washed as described above. The washed pellets were re-suspended  
276 in coaggregation buffer to achieve an optical density of 1.0 ( $\pm 0.1$ ) at 600 nm. Prior to loading the cells  
277 into the FlowCam™ device, cell suspensions were further diluted 5X in coaggregation buffer to prevent  
278 clogging of flow cell. The first species was added to the device and was pumped through until it reached  
279 the flow cell. Data collection began once the Olympus UPlanFL N 10X/0.30 objective was successfully  
280 focused on the flowing particles. The second species was added to the vessel containing the first species  
281 and gently mixed 1 minute after initiation of data collection. FlowCam™ was run for 10 minutes at a  
282 flow rate of 0.3 ml/min with images acquired at a rate of 10 frames per second. Flash duration was set  
283 to 8  $\mu$ Sec. Particle size was measured using area based diameter (ABD) and a particle filter of 5 to  
284 10000  $\mu$ m. Visual spreadsheet software was used for data collection. A minimum of 5 FlowCam runs  
285 was conducted for each pair with similar results.

286

## 287 **Acknowledgements:**

288 The authors would like to acknowledge the following funding sources: University of Michigan,  
289 Department of Epidemiology Payne Scholarship, University of Michigan Rackham One-Term Dissertation  
290 Fellowship, National Institutes of Health Interdisciplinary Program in Infectious Diseases fellowship, and  
291 The Center for Molecular and Clinical Epidemiology of Infectious Diseases.

292

## 293 **Conflict of Interest:**

294 The authors declare no conflict of interest associated with this research.

## 295 **References**

296 Arzmi, M.H., Dashper, S., Catmull, D., Cirillo, N., Reynolds, E.C. and McCullough, M., 2015.  
297 Coaggregation of *Candida albicans*, *Actinomyces naeslundii* and *Streptococcus mutans* is *Candida*  
298 *albicans* strain dependent. *FEMS yeast research*, 15(5), p.fov038.

299 Bradshaw, D., Homer, K., Marsh, P., and Beighton, D. (1994) Metabolic cooperation in oral microbial  
300 communities during growth on mucin. *Microbiology*, 140(12), pp. 3407-3412.

301 Burmølle, M., Webb, J.S., Rao, D., Hansen, L.H., Sørensen, S.J. and Kjelleberg, S., 2006. Enhanced biofilm  
302 formation and increased resistance to antimicrobial agents and bacterial invasion are caused by  
303 synergistic interactions in multispecies biofilms. *Appl Environ Microbiol*, 72(6), pp.3916-3923.

304 Busscher, H. J., & Van Der Mei, R. B. H. C. (1995). Initial microbial adhesion is a determinant for the  
305 strength of biofilm adhesion. *FEMS Microbiology Letters*, 128(3), 229–234.  
306 [http://doi.org/10.1016/0378-1097\(95\)00103-C](http://doi.org/10.1016/0378-1097(95)00103-C)

307 Cisar, J. O., Kolenbrander, P. E., & McIntire, F. (1979). Specificity of coaggregation reactions between  
308 human oral streptococci and strains of *Actinomyces viscosus* or Specificity of Coaggregation  
309 Reactions Between Human Oral Streptococci and Strains of *Actinomyces viscosus* or *Actinomyces*  
310 *naeslundii*. *Infect Immun*, 24(3), 742–752.

311 Fluid Imaging Technologies Inc. FlowCam. Particle Analysis with Vision. <http://www.fluidimaging.com/>

312 Gilbert, P., Maira-Litran, T., McBain, A. J., Rickard, A. H., & Whyte, F. W. (2002). The physiology and  
313 collective recalcitrance of microbial biofilm communities. *Adv Microb Physiol*, 46, 202.

314 Ikegami, A., Honma, K., Sharma, A., & Kuramitsu, H. K. (2004). Multiple Functions of the Leucine-Rich  
315 Repeat Protein LrrA of *Treponema denticola*. *Infect Immun*, 72(8), 4619–4627.  
316 <http://doi.org/10.1128/IAI.72.8.4619-4627.2004>

317 Jensen, H., Biggs, C., and Karunakaran, E. (2016) The importance of sewer biofilms. *WIREs Water*.  
318 doi:10.1002/wat2.1144

319 S. Katharios-Lanwermyer, C. Xi, N.S. Jakubovics & A.H. Rickard (2014) Mini-review: Microbial  
320 coaggregation: ubiquity and implications for biofilm development, *Biofouling: The Journal of*  
321 *Bioadhesion and Biofilm Research*, 30:10, 1235-1251, DOI: 10.1080/08927014.2014.976206

- 322 Kinder, S. a., & Holt, S. C. (1994). Coaggregation between bacterial species. *Methods in Enzymology*, 236,  
323 254–270. [http://doi.org/10.1016/0076-6879\(94\)36020-0](http://doi.org/10.1016/0076-6879(94)36020-0)
- 324 Kolenbrander, P. (1988). Intergeneric coaggregation among human oral bacteria and ecology of dental  
325 plaque. *Annu Rev Microbiol*, 42, 627–656. Retrieved from  
326 <http://www.annualreviews.org/doi/abs/10.1146/annurev.mi.42.100188.003211>
- 327 Kolenbrander, P. E. (2000). Oral Microbial Communities: Biofilms, Interactions, and Genetic Systems.  
328 *Annu Rev Microbiol*, 54(1), 413–437. <http://doi.org/10.1146/annurev.micro.54.1.413>
- 329 Kolenbrander, P. E., Andersen, R. N., & Moore, L. V. (1990). Intrageneric coaggregation among strains of  
330 human oral bacteria: potential role in primary colonization of the tooth surface. *Appl Environ*  
331 *Microbiol*, 56(12), 3890–3894.
- 332 Kolenbrander, P. E., Palmer, R. J., Periasamy, S., & Jakubovics, N. S. (2010). Oral multispecies biofilm  
333 development and the key role of cell-cell distance. *Nature Reviews. Microbiology*, 8(7), 471–480.  
334 <http://doi.org/10.1038/nrmicro2381>
- 335 Koop, H. M., Valentijn-Benz, M., Nieuw Amerongen, a V, Roukema, P. a, & De Graaff, J. (1989).  
336 Aggregation of 27 oral bacteria by human whole saliva. Influence of culture medium, calcium, and  
337 bacterial cell concentration, and interference by autoaggregation. *Antonie van Leeuwenhoek*,  
338 55(3), 277–290.
- 339 Ledder, R. G., Timperley, A. S., Friswell, M. K., Macfarlane, S., & McBain, A. J. (2008). Coaggregation  
340 between and among human intestinal and oral bacteria. *FEMS Microbiology Ecology*.  
341 <http://doi.org/10.1111/j.1574-6941.2008.00525.x>
- 342 Min, K. R., Zimmer, M. N., & Rickard, a H. (2010). Physicochemical parameters influencing coaggregation  
343 between the freshwater bacteria *Sphingomonas natatoria* 2.1 and *Micrococcus luteus* 2.13.  
344 *Biofouling*, 26(8), 931–940. <http://doi.org/10.1080/08927014.2010.531128>
- 345 Nagaoka, S., Hojo, K., Murata, S., Mori, T., Ohshima, T., & Maeda, N. (2008). Interactions between  
346 salivary *Bifidobacterium adolescentis* and other oral bacteria: In vitro coaggregation and  
347 coadhesion assays. *FEMS Microbiol Lett*. <http://doi.org/10.1111/j.1574-6968.2008.01092.x>
- 348 Palmer, R., Kazmerzak, K., Hansen, M., and Kolenbrander, P. (2001) Mutualism versus Independence:

- 349 Strategies of Mixed-Species Oral Biofilms In Vitro Using Saliva as the Sole Nutrient Source. *Infection*  
350 *and Immunity*, 69(9), pp. 5794-5804.
- 351 Postollec, F., Norde, W., van der Mei, H. C., & Busscher, H. J. (2005). Microcalorimetric study on the  
352 influence of temperature on bacterial coaggregation. *Journal of Colloid and Interface Science*,  
353 287(2), 461–467. <http://doi.org/10.1016/j.jcis.2005.02.030>
- 354 Rickard, a H., Leach, S. a, Buswell, C. M., High, N. J., & Handley, P. S. (2000). Coaggregation between  
355 aquatic bacteria is mediated by specific-growth-phase-dependent lectin-saccharide interactions.  
356 *Appl Environ Microbiol*, 66(1), 431–4. Retrieved from  
357 [http://www.pubmedcentral.nih.gov/articlerender.fcgi?artid=91843&tool=pmcentrez&rendertype=](http://www.pubmedcentral.nih.gov/articlerender.fcgi?artid=91843&tool=pmcentrez&rendertype=abstract)  
358 [abstract](http://www.pubmedcentral.nih.gov/articlerender.fcgi?artid=91843&tool=pmcentrez&rendertype=abstract)
- 359 Rickard, A. H., Gilbert, P., High, N. J., Kolenbrander, P. E., & Handley, P. S. (2003). Bacterial  
360 coaggregation: an integral process in the development of multi-species biofilms. *Trends Microbiol*,  
361 11(2), 94–100. [http://doi.org/10.1016/S0966-842X\(02\)00034-3](http://doi.org/10.1016/S0966-842X(02)00034-3)
- 362 Segaloff, H.E.G., Podhorez, M.E., Nemetz, M., Younger, J.G., Jakubovics, N.S., Rickard, A. H. (2014).  
363 Coaggregation between *Streptococcus gordonii* and *Streptococcus oralis* is Growth-Media  
364 Dependent. Conference paper: AADR Annual Meeting and Exhibition 2014.  
365 [https://www.researchgate.net/publication/266778750\\_Coaggregation\\_between\\_Streptococcus\\_g](https://www.researchgate.net/publication/266778750_Coaggregation_between_Streptococcus_gordonii_and_Streptococcus_oralis_is_Growth-Media_Dependent)  
366 [ordonii\\_and\\_Streptococcus\\_oralis\\_is\\_Growth-Media\\_Dependent](https://www.researchgate.net/publication/266778750_Coaggregation_between_Streptococcus_gordonii_and_Streptococcus_oralis_is_Growth-Media_Dependent)
- 367 Taweekhaisupapong, S., & Doyle, R. J. (2000). Sensitivity of bacterial coaggregation to chelating agents.  
368 *FEMS Immunol Med Microbiol*, 28(4), 343–346. [http://doi.org/10.1016/S0928-8244\(00\)00176-0](http://doi.org/10.1016/S0928-8244(00)00176-0)
- 369 Vornhagen, J., Stevens, M., McCormick, D. W., Dowd, S. E., Eisenberg, J. N. S., Boles, B. R., & Rickard, A.  
370 H. (2013). Coaggregation occurs amongst bacteria within and between biofilms in domestic  
371 showerheads. *Biofouling*, 29(1), 53–68. <http://doi.org/10.1080/08927014.2012.744395>
- 372 Watnick, P., & Kolter, R. (2000). Biofilm, city of microbes. *J Bacteriol*, 182(10), 2675–2679. Retrieved  
373 from <http://jlb.asm.org/content/182/10/2675.short>
- 374 Younes JA, van der Mei HC, van den Heuvel E, Busscher HJ, Reid G (2012) Adhesion Forces and  
375 Coaggregation between Vaginal Staphylococci and Lactobacilli. *PLoS ONE* 7(5): e36917. doi:

377

378

379

380

381

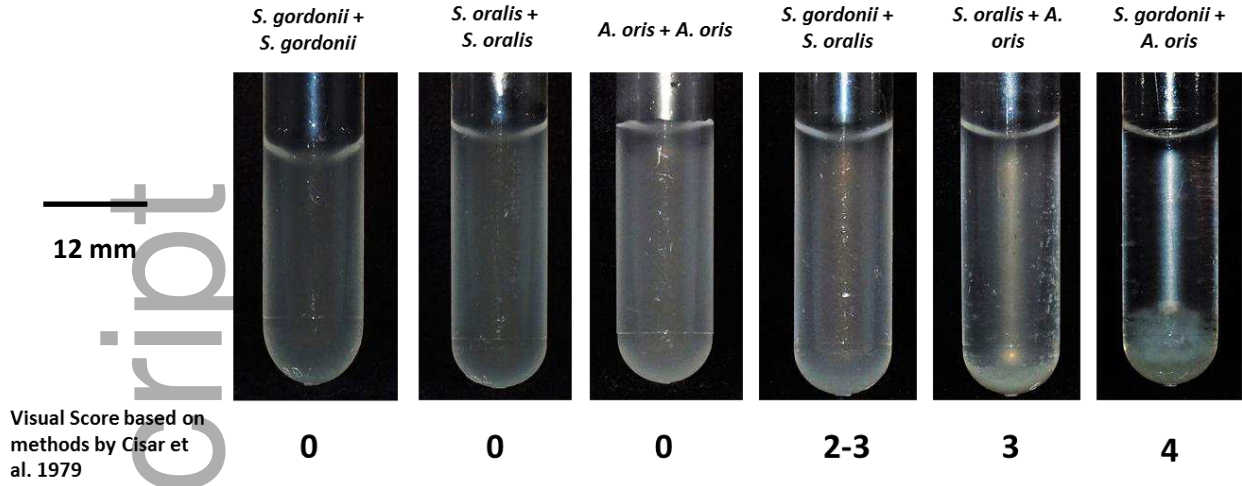
382

383 **Figures:**

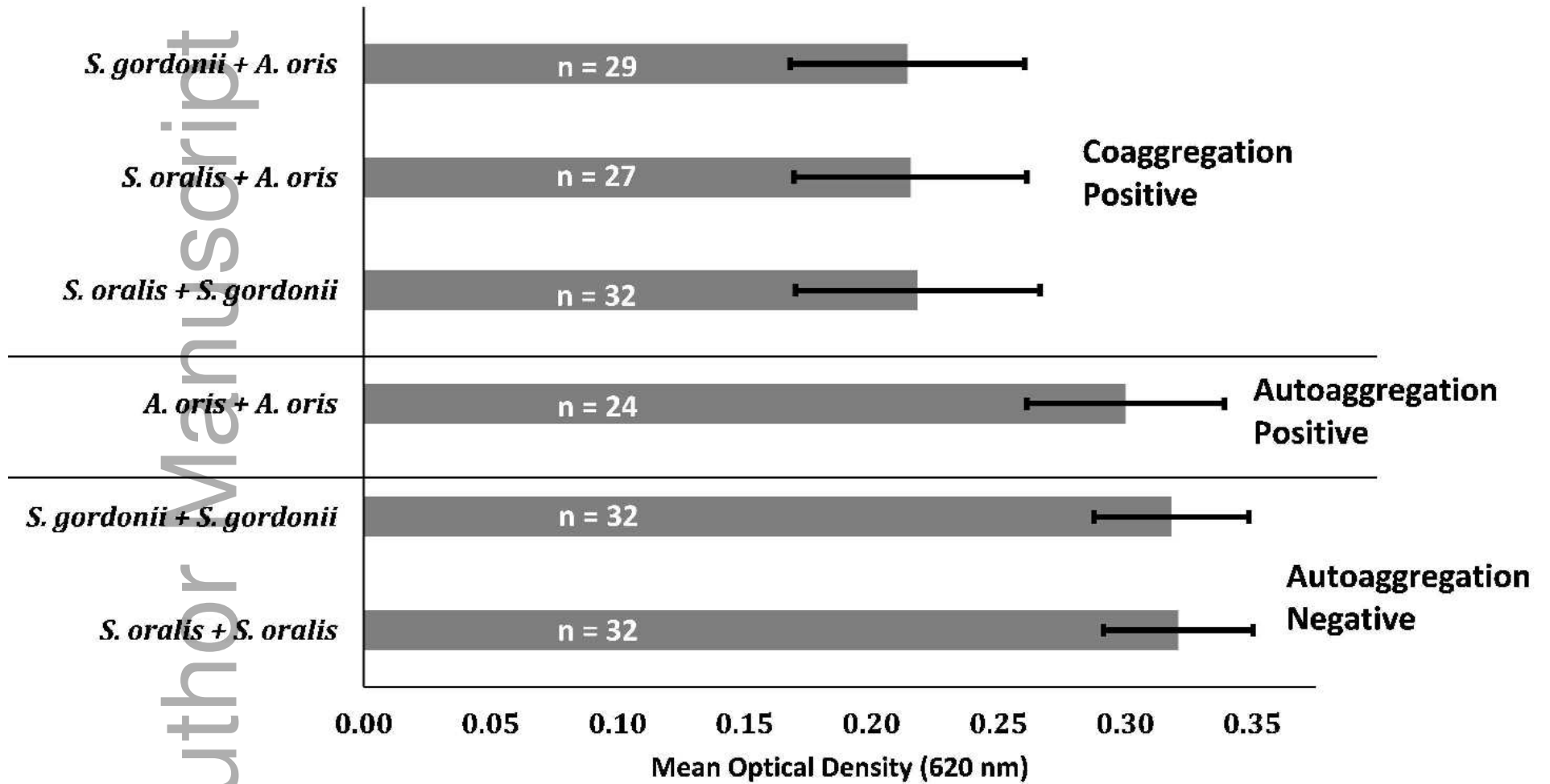
384 **Figure 1.** (A) Test crosses of pairwise combinations of *S. gordonii*, *S. oralis*, and *A. oris* with associated  
385 visual coaggregation score based on methodology by Cisar et al. 1979. (B) Mean Optical Density (620  
386 nm) of supernatant with associated 95% confidence intervals of test crosses.

387 **Figure 2.** Change in average particle area ( $\mu\text{m}$ ) per minute during 10 minute time period with associated  
388 95% confidence intervals calculated from number of particles scanned per minute for potential (A)  
389 coaggregating (*S. gordonii* + *A. oris*, *S. oralis* + *S. gordonii*, *S. oralis* + *A. oris*) and (B) autoaggregating (*S.*  
390 *gordonii*, *A. oris*, *S. oralis*) pairs as measured with the FlowCam™ device. Calculations were based on an  
391 average of 2,009 particles per minute (median = 707, maximum = 5,867, minimum = 24).

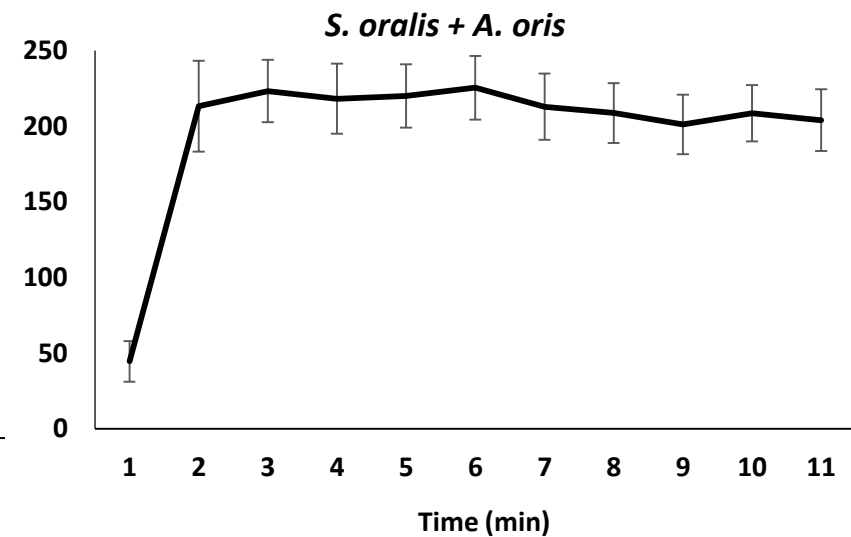
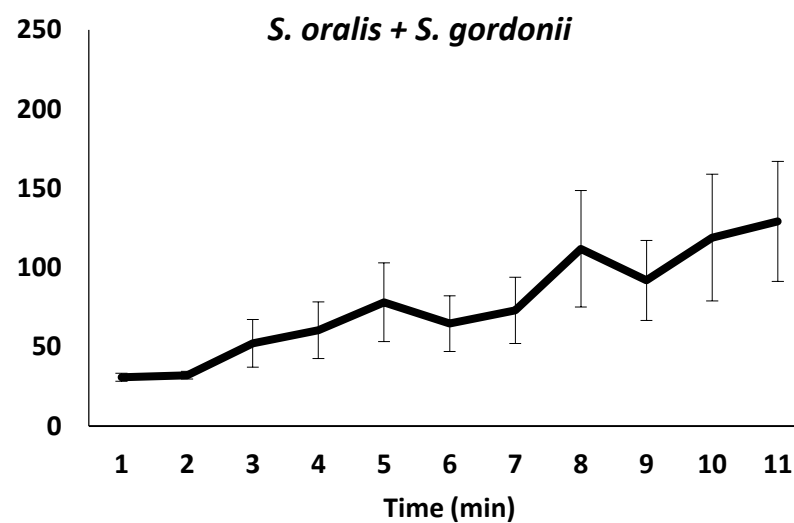
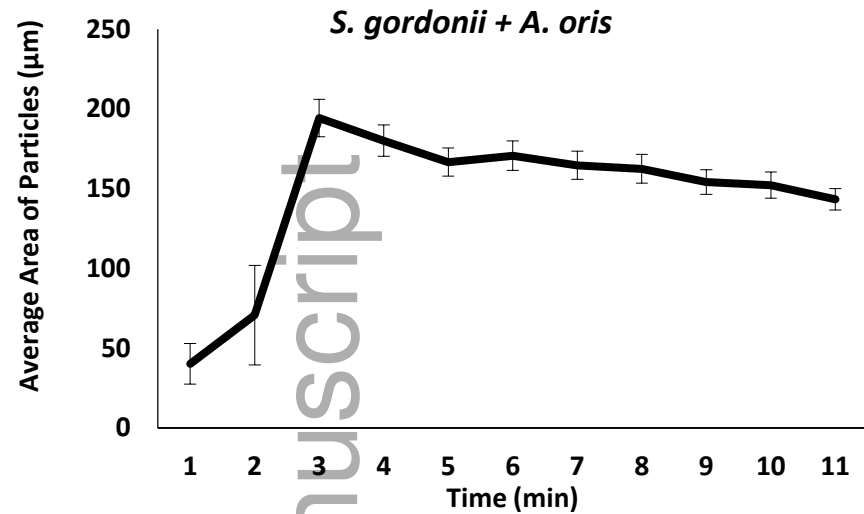
392 **Figure 3. Visualization of selection bacterial pairings using confocal microscopy.** Confocal microscopy  
393 images are represented in the x-y plane. Nucleic acid stains syto-9 (green) and syto-61 (red) was used to  
394 detect autoaggregation and coaggregation of oral microbes. Bars represent 40  $\mu\text{M}$ .



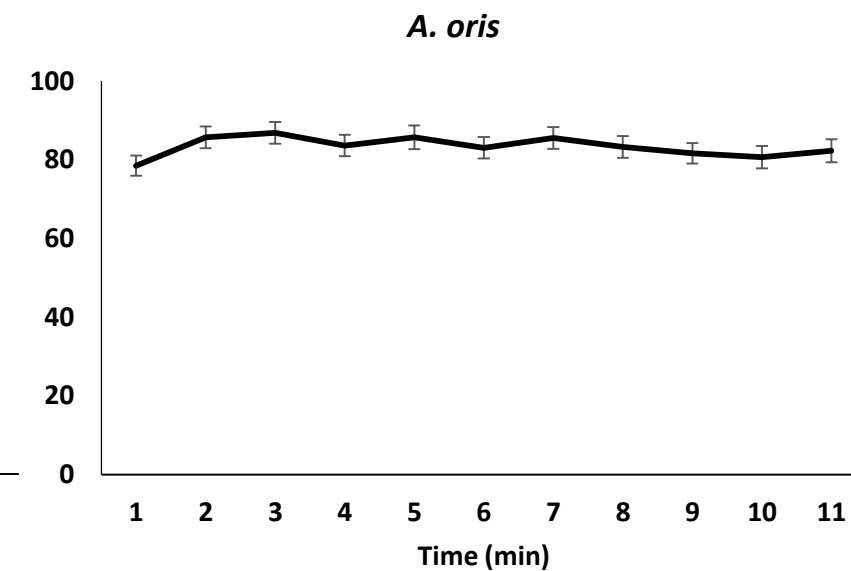
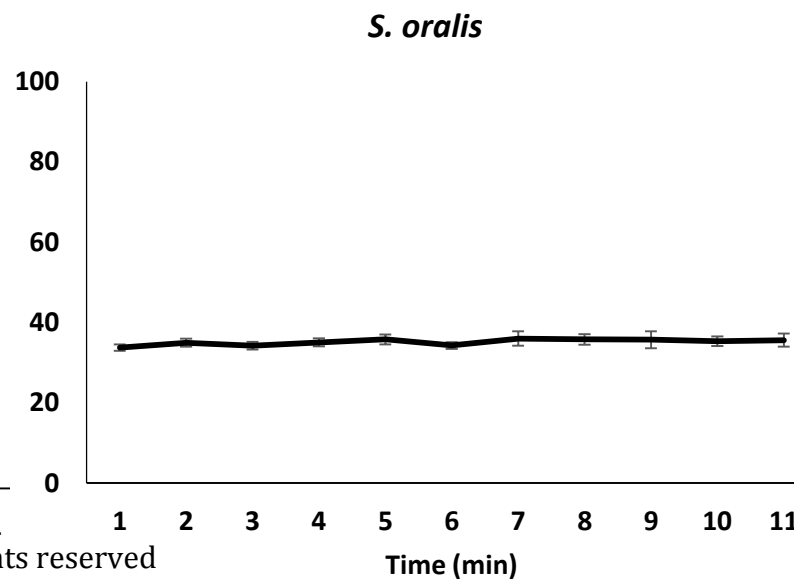
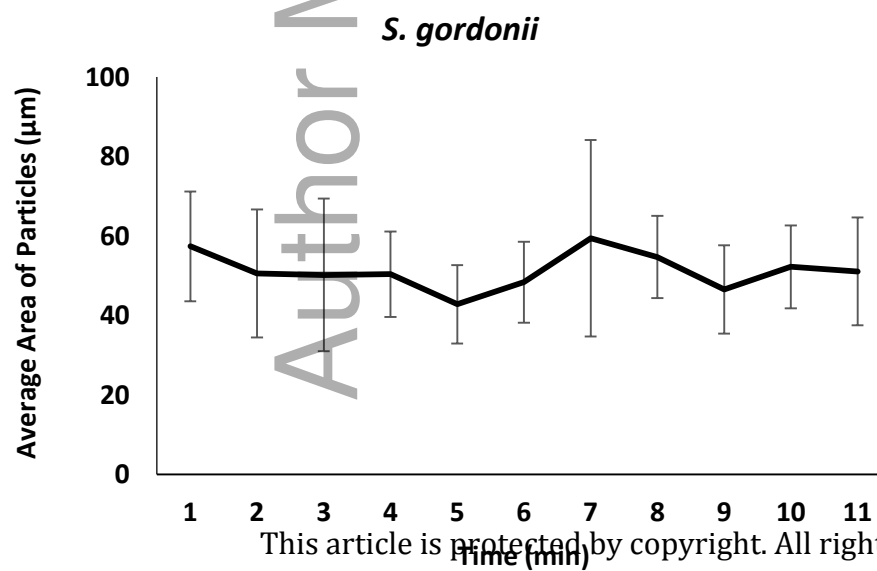


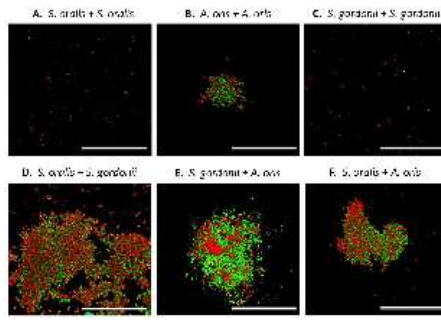


## A. Coaggregation pairings



## B. Autoaggregation pairings





lam\_12622\_f3.tiff